Proceedings of ASME Turbo Expo 2011
GT2011
June 6-10, 2011, Vancouver, British Columbia, Canada

GT2011-45796

ROTOR DYNAMIC ANALYSIS OF TIE-BOLT FASTENED ROTOR BASED ON ELASTIC-PLASTIC CONTACT

He Peng ,Zhansheng Liu ,Guilong Wang, Min Zhang
School of Energy Science and Engineering, Harbin Institute of Technology
Harbin, Heilongjiang, China

ABSTRACT

The tie-bolt fastened rotor which is assembled by rods distributed circumferentially is modeled and analyzed by finite element method with the consideration of elastic-plastic contact between discs. Based on elastic-plastic contact model between an elastic hemisphere and a rigid plane, the contact between discs is investigated by the statistical contact model of rough surfaces, and the contact stiffness is derived. The equivalent bending stiffness between discs is acquired. With the increase of the load between the two contact surfaces, the difference between the contact stiffness of purely elastic contact and elastic-plastic model is compared. With the obtained contact stiffness, the equation of motion for the tie-bolt fastened rotor system is formed and the critical speeds are calculated. It indicates that the contact stiffness between discs increases as the load increases. The contact stiffness of elastic-plastic contact model is lower than that of the elastic contact model, and the difference between the two models increases with load. With the stiffness of elastic-plastic contact, the critical speeds of tie-bolt fastened rotor are lower than that of the pure elastic contact situation.

INTRODUCTION

Tie-bolt fastened rotor is a rotor assembled by the elementary component of disc and rod. The discs are pressed together by some rods distributed circumferentially, as shown in Fig.1, or by a single rod located in the center of the rotor. In the process of assembling, the rods are elongated to offer the tighten force between discs. With the unique structure, tie-bolt fastened rotor has advantages in weight, manufacture and assembling. As tie-bolt fastened rotor is assembled by small size of parts, the cooling passages are easy to design, and the rotor can prevent large thermal stresses at high temperatures. Therefore, tie-bolt fastened rotor is widely adopted in gas turbines, especially in heavy duty gas turbines.

The assembled structure makes tie-bolt fastened rotor widely application, but it brings some difficulties in dynamical modeling and analysis of it. As there are many contact interferences between discs along the axial direction, the tie-bolt fastened rotor is not a continuous unity. The traditional methods in rotor dynamics, such as transfer matrix method and finite element method, cannot model tie-bolt fastened rotor well[1], and need many experiments to revise the prediction results. In order to model and analyze tie-bolt fastened rotor with less dependence on experiments, RaoZhushi[2] introduced a model which modeled the contact between discs as distributed springs. The discs and two ends of rotor are modeled as beams. In this model, the stiffness of the distributed springs is derived from analysis of the rough surfaces contact between discs [2-4]. This model was adopted by researchers in modeling and analyzing tie-bolt fastened rotor[5,6]. In this paper, the model introduced by RaoZhushi is applied. According to this model, the contact stiffness between discs should be obtained at first in modeling of tie-bolt fastened rotor. Therefore, the contact analysis between discs will be the first part of the modeling work.

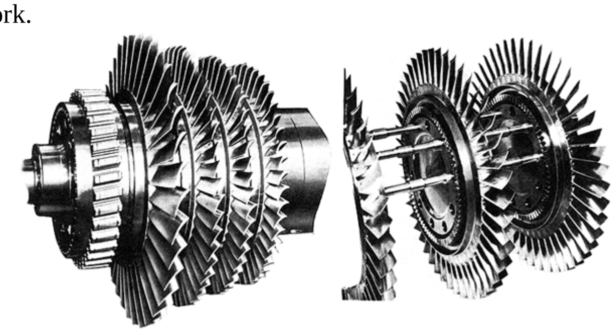

Fig. 1 The instance of tie-bolt fastened rotor (This figure is from the Internet document "Gas Turbine Operation and Maintenance Course")

The surfaces of part are not as smooth as we look in macro scale, they are inevitable roughness to some degree. Therefore, the contact between discs is actually the problem of the contact between rough surfaces. In contact mechanics, the rough surface is modeled as a rigid plane with a number of asperities or perturbations distributed on it. When two rough surfaces are pressed together, only the asperities with relative large height will interact with the other surface. As a result, only a portion of asperities will withstand the total load between rough surfaces. As we can see, the deformation behavior of single asperity is of significant importance in the analysis of rough surfaces contact. In contact mechanics, the asperity are usually supposed to be of spherical summit, the deformation of asperity can be simplified as the contact between spheres. The most famous model of the contact between two spheres is the Hertz solution, which based on the work of Hertz in 1881[7]. Hertz solution is derived from the classical elasticity theory with the assumption of the Hertz pressure distribution on the contact surface. The contact area and contact load vary with the interference of the two contact spheres. Based on Hertz work, the contact between two spheres can be equivalent to a rigid plane contact with a sphere, whose radius is the combination of the radius of former two spheres. Hertz solution plays an important part in contact mechanics, and it is still being applied in many models. However, the elastic deformation limits the application of Hertz solution. As with the increase of interference, the stresses in the elastic sphere increase at the same time. When the maximum stress in the elastic sphere reaches the yield stress of the material, the plastic deformation will appear in the elastic sphere, and then the Hertz solution will be invalid. Many research works have been done to investigate the elastic-plastic deformation of single asperity during contact[8-10]. KE elastic-plastic model, which is proposed by Kogut and Etsion, is based on the finite element analysis of a hemisphere contacting with a rigid plane, and the empirical expressions on the relations about contact area, contact load with interference are established. However, KE model is valid in a small range of interference, and will induce large deviation at large interference[9]. So Jackson and Green propose a model based on finite element analysis results with the consideration of the deformed geometry and material properties at large interference, which can describe the deformation of single asperity more accurately with various materials [9, 11]. In the work of Li, the JG model can be approximated to a simple form without lost of accuracy[12]. In the contact of tie-bolt fastened rotor, as the tighten force between discs is large, the plastic deformation would occur in the contact asperities. Therefore, the elastic-plastic contact models of single asperity will be adopted.

In the simulation of the contact between rough surfaces, the GW model is one of the most mentioned models in contact mechanics, which was proposed by Greenwood and Williamson in 1966[13]. The GW model assumes the rough surface to be a rigid plane with a large number of asperities distributed on it, and the heights of asperities vary randomly. With the assumption, the contact between rough surfaces can be modeled by the probability of the asperity with a height to be contact. So the GW model is also called statistical model. In GW model, the Hertz solution is adopted to describe the deformation behavior of single asperity during the process of contact. This indicates that, the GW model is an elastic contact model of rough surfaces. In the paper [6], the classical GW model was utilized to obtain the contact stiffness in tie-bolt fastened rotor. As the press force between discs is large, most contact asperities will deform elastic-plastically, the classical elastic GW model cannot describe the elastic-plastic deformation of asperities accurately. On the elastic-plastic contact between rough surfaces, many investigation has been done with elastic-plastic asperity contact model[14-16]. In this paper, the idea of elastic-plastic contact of rough surfaces was adopted, which used the basic GW model with the replacing of elastic Hertz solution with the elastic-plastic model of single asperity, to simulate the elastic-plastic contact between discs in tie-bolt fastened rotor.

In this paper, the models of single asperity deformation are introduced at first. Based on the elastic-plastic model of single asperity deformation, the contact between rough surfaces is modeled with the statistical model, and then the elastic-plastic contact model of rough surfaces is derived. The contact stiffness could be obtained from the contact model of rough surfaces. The tie-bolt fastened rotor is modeled in the following step, with the combination of the elastic-plastic contact stiffness between discs. The first three orders of critical speeds of tie-bolt fastened rotor are obtained, and the comparison was made between the results with consideration of elastic-plastic contact and the pure elastic contact results.

NOMENCLATURE

AA	Contact area of rough surfaces (m^2)
A	Contact area of single asperity (m^2)
A_n	Nominal contact area of rough surfaces (m^2)
$C(\upsilon)$	Ratio varies with Poisson's ratio, $\frac{8.88-10.13(\nu^2+0.089)}{6.82-7.83(\nu^2+0.0586)}$
E	Young's modulus (GPa)
G_{eq}	The equivalent bending stiffness between discs ($N{\bullet}m/rad$)
H	Hardness of material (Pa)
K	Hardness factor, $0.454+0.41\nu$
I_a	The cross sectional moment of inertia of contact surfaces (m^4)
N	Total number of the asperities on rough surfaces
PP	Contact load of rough surfaces (N)
P	Contact load of single asperity (N)
R	Radius of asperity (m)
Y	Yield stress of material (MPa)
d	Separation of rough surfaces (m)
k_n	Normal contact stiffness between rough surfaces on unit nominal contact area (N/m^3)
n	Number of contact asperities on rough surfaces
z	Height of asperity on rough surface (m)
δ	Dimensionless factor, ε_c/σ
$\phi(z)$	Distribution function of asperity heights
η	Density of asperities on nominal contact area ($1/m^2$)
σ	Standard derivation of the asperity height distribution
ν	Poisson's ratio
ε	Interference of single asperity (m)

Superscripts

*	Dimensionless values

Subscripts

GW	The values of GW model
c	The values at critical interference of single asperity
e	The elastic deformation of single asperity
$P1$	The value of first elastic-plastic deformation region
$P2$	The value of second elastic-plastic deformation region
1	The values of sphere 1
2	The values of sphere 2

ANALYSIS OF CONTACT BETWEEN DISCS

The surfaces of parts are rough to some degree in micro scale. Therefore, the contact between discs is actually the contact between two rough surfaces. In this section, the contact between discs is modeled and analyzed. As the deformation behavior of single asperity during contact is the base of the contact analysis, the model of a single asperity deformation behavior is introduced at first.

The model of single asperity deformation

The model of a single asperity deformation behavior during contact behavior is of significant importance in contact mechanics, as it describes the basic relations between contact area, contact load and interference. In contact mechanics, the asperity is usually modeled as spheres. Based on the work of Hertz, the contact between two spheres can be treated as the contact between a sphere and a rigid plane, where the sphere radius is the combination of the radius of former two spheres. As the deformation mainly occurs at the summit of the sphere, the contact of asperity is usually simplified as an elastic hemisphere contact with a rigid plane, which is shown in Fig.2. The simplified model of single asperity is adopted mainly in the research work on modeling of single asperity contact.

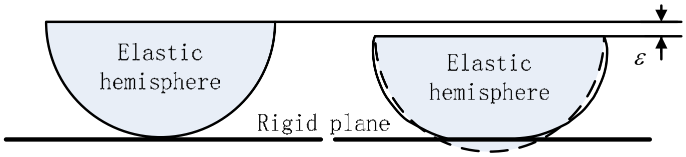

Fig. 2 The spherical contact model

As the model illustrated in Fig.2, the deformation of the elastic hemisphere increases as the interference ε increase. During the processes of the interference increases from 0 to the critical interference ε_c, the hemisphere deforms elastically. Here the critical interference indicates the transition of elastic deformation to plastic deformation, which judged from the stress analysis in the hemisphere.

According Hertz solution, in the elastic regime of deformation, contact load P_e can be written as

$$P_e = \frac{4}{3} E R^{\frac{1}{2}} \varepsilon^{\frac{3}{2}} \tag{1}$$

Where R is the radius of the elastic hemisphere, which is the combination of the radius R_1, R_2, of the two contact spheres with $\frac{1}{R} = \frac{1}{R_1} + \frac{1}{R_2}$; E is the equivalent Young modulus, $\frac{1}{E} = \frac{1-\nu_1^2}{E_1} + \frac{1-\nu_2^2}{E_2}$,with E_1, E_2 and ν_1, ν_2 are the Young modulus and Poisson's ratio of the materials of the two contact spheres respectively.

The critical interference ε_c is an important parameter in the contact model of a single asperity. It depends on the properties of the material and the geometric parameters of the hemisphere. The expression of critical interference derived by Chang et al, is applied in the elastic-plastic analysis of a single asperity widely [14]. It is written as:

$$\varepsilon_c = \left(\frac{\pi K H}{2E} \right)^2 R \tag{2}$$

Where K relates to Poisson's ratio of the material yield first, is given by $K = 0.454 + 0.41\nu$; H is the hardness of the material, it can be written by $H = 2.8Y$, and Y is the yield stress of the material; E and R are the equivalent Young modulus and radius of the elastic hemisphere respectively.

When the interference ε passes the critical interference ε_c, in some region of the hemisphere, the stress becomes larger than the yield stress of the material. As a result, the plastic deformation occurs in the hemisphere. According to finite element analysis by Kogut and Etsion, when the interference in the region of $\varepsilon_c \le \varepsilon \le 6\varepsilon_c$, the deformation of the hemisphere summit is still dominated by elastic deformation, plastic deformation is only a small portion in the hemisphere summit. The situation is changed after the interference reaches $6\varepsilon_c$, when the plastic deformation expends to the outside surface of the hemisphere, and dominates the deformation of the hemisphere summit. With the finite element analysis results, the relation between contact and interference can be written as[8]:

$$\begin{cases} P_{p1} = P_C \cdot 1.03 \left(\dfrac{\varepsilon}{\varepsilon_C} \right)^{1.425} & 1 \le \dfrac{\varepsilon}{\varepsilon_c} \le 6 \\ P_{p2} = P_C \cdot 1.40 \left(\dfrac{\varepsilon}{\varepsilon_C} \right)^{1.263} & 6 \le \dfrac{\varepsilon}{\varepsilon_c} \le 110 \end{cases} \tag{3}$$

The KE model use a piecewise function to describe the evaluation of the plastic deformation from as the interference varies in the region $\varepsilon_c \le \varepsilon \le 110\varepsilon_c$. When the interference exceeds $110\varepsilon_c$, KE model cannot predict the contact load accurately. Jackson and Green extend the range of interference with the consideration of varied geometry and material dependence at large interference. Based on the finite element analysis, they also propose an empirical formulation [9]. The JG model can describe the deformation of single asperity form elastic-plastic to fully plastic regime. In the work of L.Li[12], the JG model is simplified to describe the deformation at large interference. The simplified JG model can be written as:

$$P_{SJG} = P_c \cdot 4.6C(\upsilon)\left(\frac{\varepsilon}{\varepsilon_c}\right) \tag{4}$$

Where $C(\upsilon) = \dfrac{8.88 - 10.13(\nu^2 + 0.089)}{6.82 - 7.83(\nu^2 + 0.0586)}$ relates the Poisson's ratio of the material yield first.

It is convenient to introduce the dimensionless form of the single asperity contact model. The interference, contact area and contact load are normalized by the values at critical interference, respectively. The dimensionless procedure can be written as:

$$\varepsilon^* = \frac{\varepsilon}{\varepsilon_c}, P^* = \frac{P}{P_c} \tag{5}$$

The relationship of contact load and interference in the Hertz solution, KE model and simplified JG model can be expressed in the dimensionless form as follows.

The dimensionless load by Hertz solution:

$$P^* = \left(\varepsilon^*\right)^{\frac{3}{2}} \tag{6}$$

The dimensionless contact load of KE model:

$$\begin{cases} P_{p1}^* = 1.03\left(\varepsilon^*\right)^{1.425} & 1 \le \varepsilon^* \le 6 \\ P_{p2}^* = 1.40\left(\varepsilon^*\right)^{1.263} & 6 \le \varepsilon^* \le 110 \end{cases} \tag{7}$$

The dimensionless contact load of simplified JG model:

$$P_{SJG}^* = 4.6C(\upsilon)\left(\frac{\varepsilon}{\varepsilon_c}\right) \tag{8}$$

Where $P_e^*, P_{p1}^*, P_{p2}^*, P_{SJG}^*$ are the dimensionless contact loads in the different regions of interferences.

The differences between the Hertz solution and elastic-plastic model can be illustrated in the figures bellow.

When the interference varies in the region $0 \le \varepsilon \le 110\varepsilon_c$, the contact load of Hertz solution, KE model and JG model are plotted in Fig.3. As the KE model and the JG model use Hertz solution in the elastic regime, the three models are consistent at small interference. However, at large interference, the plastic deformation induces the KE model and the JG model predicts smaller contact load than the Hertz solution, the discrepancy increases as the interference increases. As the KE model and the JG model all consider the plastic deformation, they are in accordance with each other when the interference in the range $0 \le \varepsilon \le 110\varepsilon_c$.

The contact load of Hertz solution, simplified JG model and JG model are plotted in Fig.4, while the contact interference in the region $110\varepsilon_c \le \varepsilon$. The Hertz solution predicts large contact loads than the two models, and the difference increases a lot with the increase of interference. The contact load of the simplified JG model and the JG model are consistent, the difference can be neglect.

From the comparison of the contact load of the different single asperity deformation models, the consideration of plastic deformation will result in significantly difference to elastic deformation in heavily load situation. In the region $0 \le \varepsilon \le 110\varepsilon_c$, the KE model and the JG model are consistent, and in the region $110\varepsilon_c \le \varepsilon$, the simplified JG model is in accordance with JG model.

In this paper, the KE model is adopted to describe deformation as the interference in the region $\varepsilon_c \le \varepsilon \le 110\varepsilon_c$, and the simplified JG model is applied at large interferences.

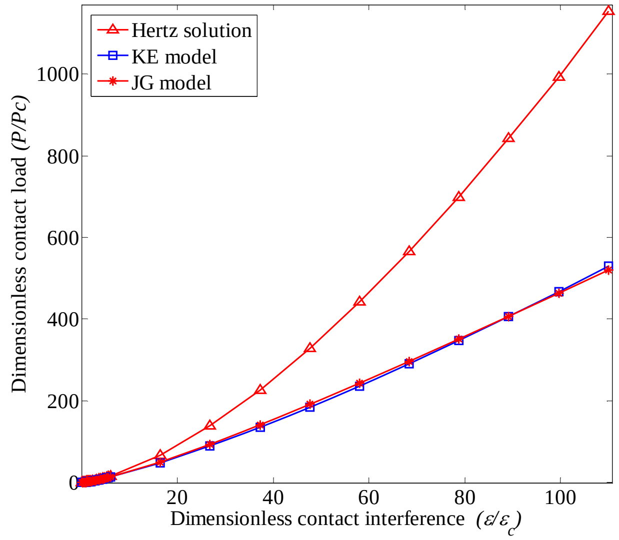

Fig. 3 Contact loads of the different single asperity deformation models at small interference

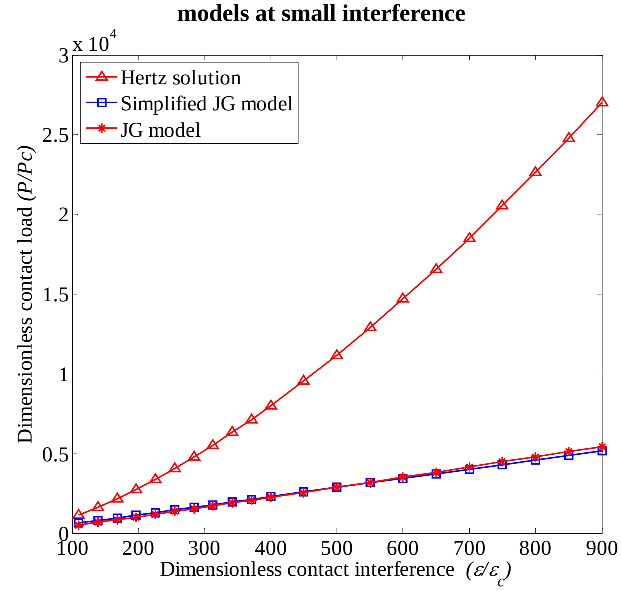

Fig. 4 Contact loads of the different single asperity deformation models at large interference

Modeling of the contact between two rough surfaces

With the analysis of a single asperity model, the contact between rough surfaces can be modeled and analyzed. Based on the work of Greenwood and Tripp[17], the contact between two rough surfaces can be equivalent to the contact between a rough surface and a rigid plane, which simplifies the problem significantly. In this section, the contact between two rough surfaces is modeled based on statistical contact model.

In the statistical contact model, the rough surface is considered as a nominal flat plane with a large number of asperities distributed on it. All the asperity summits are spherical, with the same radius. The height z of the asperities varies randomly, with the probability density function $\phi(z)$. Therefore, the probability of an asperity with height between z and dz is $\phi(z)dz$. Suppose a rough surface contacting with a rigid smooth surface, the distance of the rigid surface of the rough surface and the other rigid surface is d, and the asperities on the rough surface with height larger than d will contact with the rigid surface, as shown in Fig.5. If the number of the asperities on the rough surface is N, the number of the asperities contact with the rigid surface is $n = N\int_d^\infty \phi(z)dz$. Then the contact interference ω of a contact asperity with height z is equal to $z-d$. With the combination of the single asperity contact model, the contact area and contact load of the rough surface can be derived.

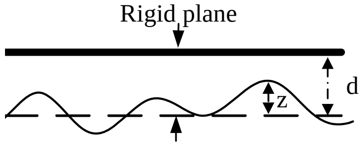

Fig. 5 Schematic of contact between a rigid plane and a rough surface

The classical GW model is the origin of the statistical model. However, the GW model adopts Hertz solution to describe the deformation of a single asperity, which indicates the GW model is limited as the elastic contact model of rough surfaces. The contact load of GW model is written as:

$$P_{GW} = \frac{4}{3}NER^{\frac{1}{2}}\int_d^\infty (z-d)^{\frac{3}{2}}\phi(z)dz \tag{9}$$

In this paper, the elastic-plastic modeling of discs is based on statistical model, with the application of elastic-plastic model of a single asperity deformation.

In elastic-plastic model introduced in the last section, the process of a single asperity deformation is divided into four sections: elastic deformation with $0<\varepsilon\le\varepsilon_c$; elastic-plastic deformation with $\varepsilon_c\le\varepsilon\le 6\varepsilon_c$; elastic-plastic deformation with $6\varepsilon_c\le\varepsilon<110\varepsilon_c$ and elastic-plastic deformation at large interference $110\varepsilon_c\le\varepsilon$. With the ideas of statistical model of rough surfaces contact, the probability of an asperity with height z on the rough surface contacting with the rigid plane is $\int_d^\infty \phi(z)dz$, and the probabilities of the deformation of the asperity in each region of the elastic-plastic model are $\int_d^{d+\varepsilon_c}\phi(z)dz$, $\int_{d+\varepsilon_c}^{d+6\varepsilon_c}\phi(z)dz$, $\int_{d+6\varepsilon_c}^{d+110\varepsilon_c}\phi(z)dz$ and $\int_{d+110\varepsilon_c}^{\infty}\phi(z)dz$ respectively. Supposed there are N asperities on the rough surface in all, the numbers of the asperities deformed in the four regions of the elastic-plastic model are N_e, N_{p1}, N_{p2} and N_{SJG} respectively. Based on statistical model, it can be derived that $N_e = N\int_d^{d+\varepsilon_c}\phi(z)dz$, $N_{p1} = N\int_{d+\varepsilon_c}^{d+6\varepsilon_c}\phi(z)dz$, $N_{p2} = N\int_{d+6\varepsilon_c}^{d+110\varepsilon_c}\phi(z)dz$ and $N_{SJG} = \int_{d+110\varepsilon_c}^{\infty}\phi(z)dz$.

Based on the contact load formulation of the single asperity elastic-plastic deformation model, the expected contact load of rough surface can be expressed as follows.

$$\begin{aligned} PP &= N\int_d^{d+\varepsilon_c} P_e\phi(z)dz + N\int_{d+\varepsilon_c}^{d+6\varepsilon_c} P_{p1}\phi(z)dz \\ &+ N\int_{d+6\varepsilon_c}^{d+110\varepsilon_c} P_{p2}\phi(z)dz + N\int_{d+110\varepsilon_c}^{\infty} P_{SJG}\phi(z)dz \end{aligned} \tag{10}$$

The four parts on the right side of the expression indicate the contribution of the four regions of deformation.

The total number of the asperities on a rough surface can be written as $N=\eta A_n$, where η is the surface density of asperities on nominal contact surface, A_n is the area of nominal contact surface. The Gaussian distribution function is a good approximation for many surfaces, so the distribution of asperities on rough surfaces can be written as $\phi(z) = \frac{1}{\sqrt{2\pi}\sigma}e^{-\frac{1}{2}\left(\frac{z}{\sigma}\right)^2}$, where σ is the standard deviation of the asperities height distribution on rough surface.

It is convenient to normalize the model to dimensionless variables. In this paper, the length variable is normalized by the standard deviation of the asperities height distribution. Then the contact model can be normalized as:

The dimensionless contact load of GW model:

$$PP_{GW} = \frac{4}{3}\eta A_n ER^{\frac{1}{2}}\sigma^{\frac{3}{2}}\int_h^\infty (s-h)^{\frac{3}{2}}\phi^*(s)ds \tag{11}$$

The dimensionless contact load of elastic-plastic contact model:

$$PP^* = \frac{4}{3}\eta A_n ER^{\frac{1}{2}}\varepsilon_c^{\frac{3}{2}}\begin{bmatrix} \delta^{-\frac{3}{2}}\int_h^{h+\delta}(s-h)^{\frac{3}{2}}\phi^*(s)ds \\ +1.03\delta^{-1.425}\int_{h+\delta}^{h+6\delta}(s-h)^{1.425}\phi^*(s)ds \\ +1.40\delta^{-1.263}\int_{h+6\delta}^{h+110\delta}(s-h)^{1.263}\phi^*(s)ds \\ +4.6C(\upsilon)\delta^{-1}\int_{h+6\delta}^{h+110\delta}(s-h)\phi^*(s)ds \end{bmatrix} \tag{12}$$

Where $\phi^*(s) = \frac{1}{\sqrt{2\pi}}e^{-\frac{1}{2}s^2}$ is the dimensionless distribution function , $C(\upsilon) = \frac{8.88-10.13(\nu^2+0.089)}{6.82-7.83(\nu^2+0.0586)}$ and $\delta = \frac{\varepsilon_c}{\sigma}$.

Based on the expression of contact load between rough surfaces, the contact stiffness on unit nominal contact area can be derived by the definition of stiffness:

$$k_n = \frac{d(PP^*)}{A_n d(h)} \tag{13}$$

The elastic contact stiffness based on GW model and the elastic-plastic contact stiffness can be obtained respectively.

The contact stiffness on unit area of nominal contact surface derived by GW model is:

$$k_{nGW} = 2\eta E R^{\frac{1}{2}} \sigma^{\frac{1}{2}} \int_h^\infty (s-h)^{\frac{1}{2}} \phi^*(s) ds \tag{14}$$

The contact stiffness on unit area of nominal contact surface derived by elastic-plastic contact of rough surfaces is:

$$k_{nE-P} = \frac{4}{3}\eta E R^{\frac{1}{2}} \varepsilon^{\frac{1}{2}} \begin{bmatrix} \frac{3}{2}\delta^{-\frac{1}{2}} \int_h^{h+\delta} (s-h)^{\frac{1}{2}} \phi^*(s) ds \\ +1.03*1.425\delta^{-0.425} \int_{h+\delta}^{h+6\delta} (s-h)^{0.425} \phi^*(s) ds \\ +1.40*1.263\delta^{-0.263} \int_{h+6\delta}^{h+110\delta} (s-h)^{0.263} \phi^*(s) ds \\ +4.6C(\upsilon) \int_{h+6\delta}^{h+110\delta} \phi^*(s) ds \end{bmatrix} \tag{15}$$

With the contact stiffness on unit area of nominal contact surface, tie-bolt fastened rotor can be modeled and analyzed.

MODELING OF TIE-BOLT FASTENED ROTOR

A tie-bolt fastened rotor model is illustrated in Fig.6. There are twenty discs and two ends, which are tightened by eight rods distributed circumferentially. Based on the contact models introduced, the contact between discs can be modeled by the mechanical model proposed by RaoZhushi [2].

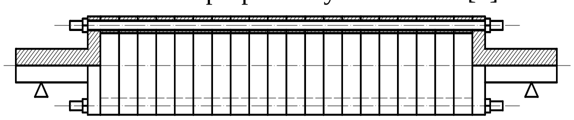

Fig. 6 Schematic of the tie-bolt fastened rotor

In the mechanical model, the contact between the two contact discs' surfaces is represented by distributed springs, which stiffness can be obtained by the contact analysis with the model mentioned above. In the modeling of rotor, the bending stiffness between the contacting discs is required. Therefore, the distribution spring should be equivalent to the bending stiffness.

The equivalent bending stiffness of the contact surfaces can be obtained by the following formulation.

$$G_{ep} = k_n I_a \tag{16}$$

Where I_a the cross sectional moment of inertia of contact surfaces.

The mechanical model is shown in Fig.7.

With the equivalent bending stiffness between the contact surfaces, the tie-bolt fastened rotor can be modeled by finite element method. The two ends and discs are modeled as Timoshenko beam, and the contact is modeled as a bending spring which connects the two nodes on the two contact surfaces respectively.

The mass matrix $[M]$ and the stiffness matrix $[K]$ can be obtained by assembling the relative matrix of discs and springs. The stiffness matrix $[K]$ should be reminded. As the contact between discs only transfers the forces, the contribution of the contact mainly on the stiffness matrix of tie-bolt fastened rotor, and the influence on the mass is negligible. Therefore, the stiffness matrix $[K]$ includes the matrixes of the discs and the two ends, as well as the matrix of the contact equivalent bending stiffness. In the forming of the stiffness matrix, the stiffness matrix of discs and ends are assembled directly, and the matrix of the bending stiffness is added at the interface of the discs and ends, which represents the effect of contact. However, the mass matrix $[M]$ is same as the directly combination of each disc and end.

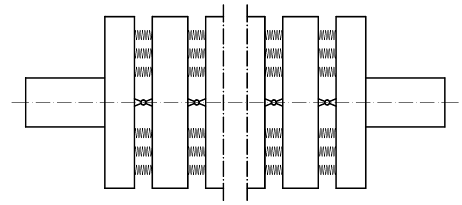

(a)

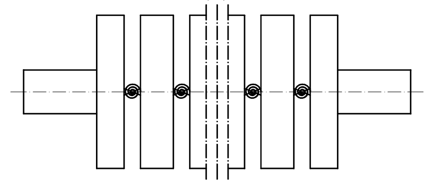

(b)

Fig. 7 The mechanical model by RaoZhushi (a) the equivalent distribute springs between contact surfaces; (b) the equivalent bending stiffness between contact surfaces

With the model of tie-bolt fastened rotor, the critical speeds can be acquired.

RESULTS AND DISCUSSION

In this section, a tie-bolt fastened rotor was modeled and analyzed. The sketch of the tie-bolt fastened rotor model is shown in Fig.8.

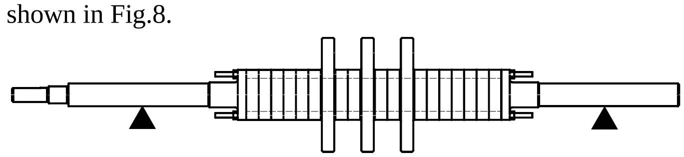

Fig. 8 The tie-bolt fastened rotor model

There are seventeen small discs, three big discs and two ends, and all of them are tightened by eight rods circumferentially. The discs are the ones in Rao's work [2], so the statistical parameters of the contact surfaces of discs are adopted in this paper. The statistical parameters in Rao's work are listed in Table 1.

Table 1 The statistical parameters in Rao's work

σ	2.01 μm
R	95 μm
η	$5.625E7\ 1/m^2$

First of all, the contact between discs is modeled and analyzed. As the integration in the formulation of contact area and contact load cannot be solved analytically, the numerical method is applied. In the assembling process of tie-bolt fastened rotor, the tighten force between discs is assigned at first. Therefore, in the simulation of the contact, the total tighten force between rough surfaces is provided, while the separation and the real contact area can be obtained by the models of the rough surfaces contact. The results of the analysis of the rough surfaces contact are plotted in the following figures.

The dimensionless separation between the reference planes of the two contacting rough surfaces under various tighten forces is plotted in Fig.9 and Fig.10. The separation of the elastic contact is larger than the elastic-plastic contact under the same tighten force, the discrepancy of the separation increases with the increment of the tighten force. The difference of the separation between elastic contact and elastic-plastic contact results from that the plastic deformation makes the asperity softer than the elastic situation. From Fig.9, it can be found that when the contact load decreases to zero, the separations of elastic contact and elastic-plastic contact all tend to be infinite. It results from the theory of statistical contact model. As the zero contact load relates to no asperity on the rough surfaces interact with the rigid plane, only the asperity with infinite height has zero probability to interact with the rigid plane, and this relates to the infinite separation.

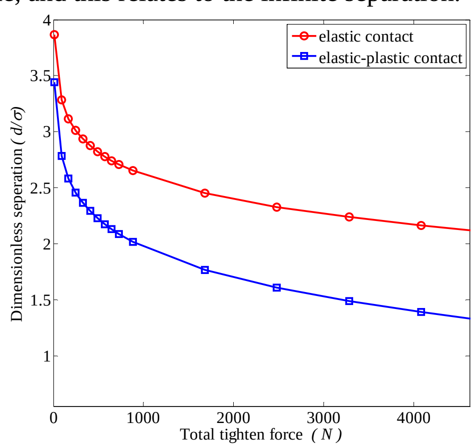

Fig. 9 the separation between rough surfaces under low load

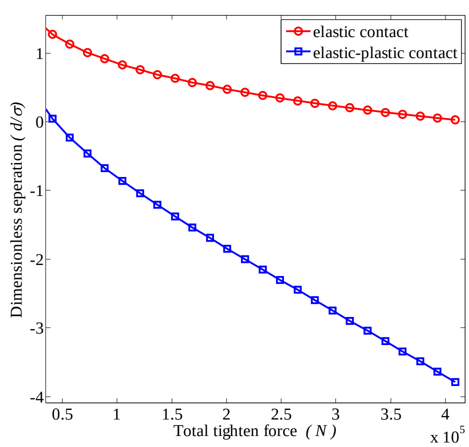

Fig. 10 The separation between rough surfaces under high load

The contact stiffness on unit area of nominal contact surface and the equivalent bending stiffness between discs can be obtained. As shown in Fig.11, the normal contact stiffness between discs of the elastic model is larger than the elastic-plastic contact model, and the discrepancy of the two models increases with the increment of the tighten force. The equivalent bending stiffness has the same trend as the normal contact stiffness, as shown in Fig.12. It is due to the equivalent bending stiffness is linear with normal contact stiffness. This is reasonable as under small tighten forces, the plastic deformation plays little part in the whole deformation, and the differences of the two models are small. However, under large tighten forces, the plastic deformation increases and becomes dominant in the total deformation, the stiffness of the elastic-plastic model becomes much smaller than the elastic model.

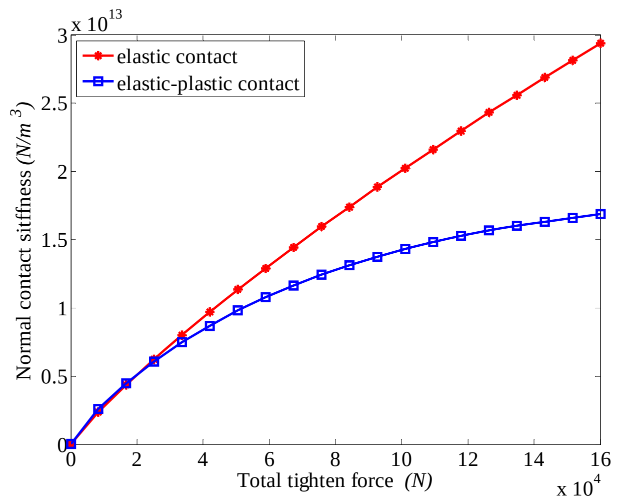

Fig. 11 The normal contact stiffness on unit nominal contact surface

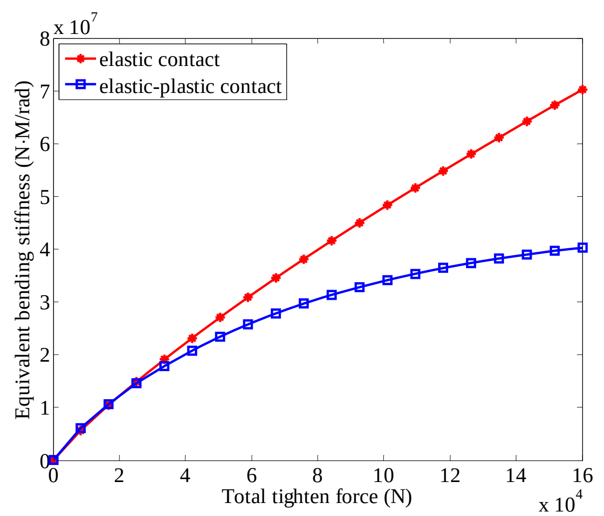

Fig. 12 The equivalent bending stiffness

With the equivalent bending stiffness between the contacts of discs, the tie-bolt fastened rotor is modeled by the method introduced above, and the critical speeds of the tie-bolt fastened rotor are obtained. As the equivalent bending stiffness varied with the tighten force, the critical speeds can be obtained under a series of tighten forces. The first three orders of critical speeds for the tie-bolt fastened rotor model are plotted in the following figures. The results of elastic contact and the elastic-plastic are all plotted in a figure. In order to illustrate the difference between the tie-bolt fastened rotor and the continuous rotor, the critical speeds of a continuous rotor with the same size of the tie-bolt fastened rotor are computed and plotted as well.

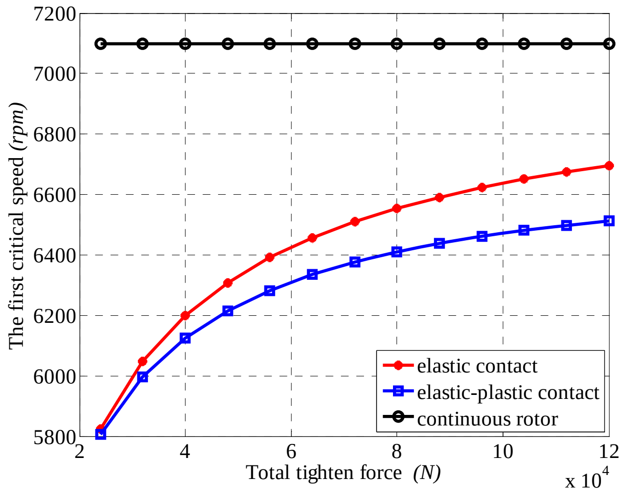

Fig. 13 The first critical speed under various conditions

As the critical speeds plotted in figs.13-15, the first three orders of the critical speeds has the same variation trend with the increase of tighten force. The critical speeds of the tie-bolt fastened rotor are much smaller than the continuous rotor, even the tighten force is sufficiently large. The critical speeds of the tie-bolt fastened rotor increase with the tighten force, while the increase becomes more slow with the increment of the tighten force. This can be explained by the increase trend of the contact stiffness with tighten forces. The critical speeds of tie-bolt fastened rotor with elastic contact are larger than the elastic-plastic contact situation.

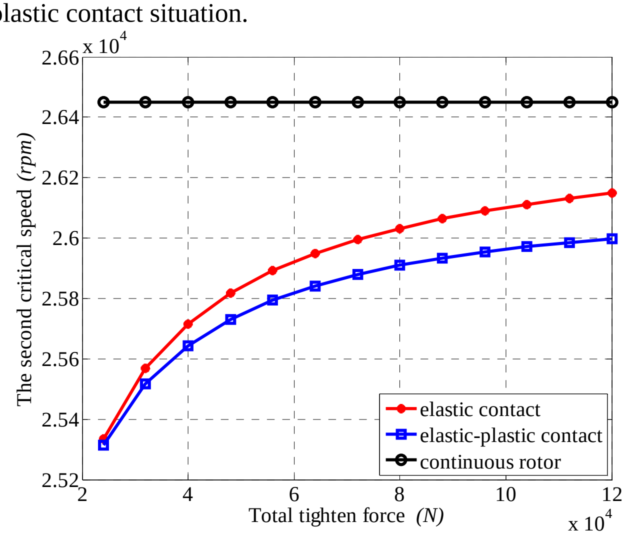

Fig. 14 The second critical speed under various conditions

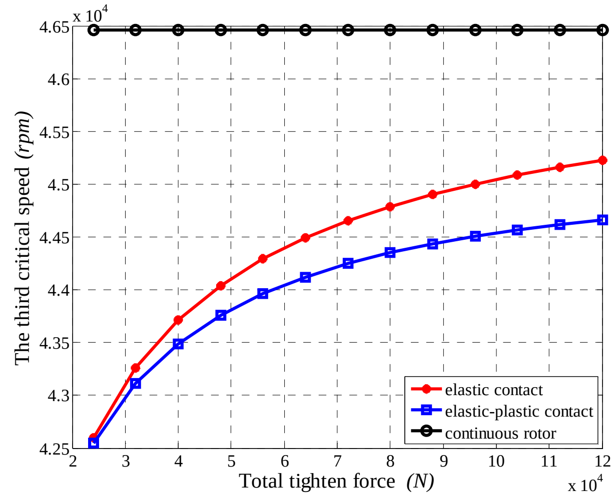

Fig. 15 The third critical speed under various conditions

The discrepancy of the critical speeds with the two contact stiffness is negligible at small tighten forces, while it increases to be constant with the growth of the tighten force. The current discrepancy of critical speeds is due to the trend of the stiffness the two models with the incerase of total tighten force. As the elastic-plastic contact model considered the plastic deformation of the asperities on the contacting rough surfaces, it is of greater fidelity in describing the contact effects between discs , and a more accurate model in predicting the critical speeds of tie-bolt fastened rotor should be considered.

CONCLUSIONS

The elastic-plastic contact of tie-bolt fastened rotor discs were modeled based on the elastic-plastic single asperity deformation model, and the stiffness of elastic-plastic contact was obtained. The tie-bolt fastened rotor was modeled with the elastic-plastic contact stiffness, and the critical speeds were computed. The comparison of the elastic contact and the elastic-plastic contact between discs were carried out.

Results shows that, as the consideration of the asperity plastic deformation on rough surfaces, the elastic-plastic model has greater fidelity in describing the contact behavior of rough surfaces to elastic model, and the critical speeds of tie-bolt fastened rotor predicted by elastic-plastic contact should be more precise than the elastic contact results.

ACKNOWLEDGMENTS

This paper is supported by 863 grant of Ministry of Science and Technology, China.

REFERENCES

[1] L.M. Shi, Y.C Zhang, 2007, “Model test and analysis of gas turbine rotor,” Gas Turbine Technology, 20(4), pp. 47-49.

[2] Z.S. Rao, 1992, “A Study of Dynamic Characteristics and Contact Stiffness of the Rod Fastening Composite Special Rotor”, Ph.D. thesis, Harbin Institute of Technology.

[3] Z.S. Rao, S.B. Xia and G.M Wang, 1994, "A Study of Contact Stiffness of Flat Rough Surfaces," Journal of Mechanical Strength, 16(2), pp. 72-76.
[4] Z.S. Rao, S.B. Xia and G.M. Wang, 1996, "Experimental Modal Analysis and Computation for Special Kind of Composite Rotor System," Journal of Vibration and Shock, 15(1), pp. 68-70.
[5] L.M. Shi, Y.C. Zhang, 2008, "The Measurement and Calculation Analysis of Natural Frequencies for Tie-bolt fastened rotors," Journal of Vibration and Shock, 28(S), pp. 47-49.
[6] Yuan Qi, Gao Rui, Feng Zhenping, Wang Jianlu, 2008, "Analysis of Dynamic Characteristics of Gas Turbine Considering Contact Effects and Pre-tightening Force", Proceedings of ASME Turbo Expo, Berlin, Germany,GT2008-50396.
[7] Timoshenko, S.P., and Goodier,1970, Theory of Elasticity, 3rd ED., MacGraw-Hill, New York, Chap. 12.
[8] L. Kogut, I. Etsion, 2002, "Elastic-Plastic Contact Analysis of s Sphere and a Rigid Flat," Journal of Applied Mechanics, 69, pp. 657-662.
[9] Robert L. Jackson, Itzhak Green, 2005, "A Finite Element Study of Elasto-Plastic Hemispherical Contact Against a Rigid Flat", Journal of Tribology, 127, pp. 343-354.
[10] S. Shankar, M.M. Mayuram, 2008, "A Finite Element Based Study on the Elastic-Plastic Transition Behavior in a Hemisphere in Contact With a Rigid Flat," Journal of Tribology, 130，(044502)1-(044502)6.
[11]Quicksall, J.J., Jackson, R.L. and Green,I. "Elasto-plastic Hemispherical Contact Models for Various Mechanical Properties," Proceedings of the Institude of Mechanical Engineers, Journal of Engineering Tribology, 218,(J06503)313-322.
[12] L.Li, I.Etsion, and F.E. Talke, 2010, "Contact Area and Static Friction of Rough Surfaces With High Plasticity Index," Journal of Tribology, 132, (031401)1-(031401)10.
[13] Greenwood, J.A., and Williamson, J.B.P., 1966, "Contact of Nominally flat Surfaces," Proc, R. Soc. London, 295, pp. 300-319.
[14] Chang, W.R., Etsion, I., and Bogy, D.B., 1987, "An Elastic-Plastic Model for the Contact of Rough Surfaces," ASME J. Tribol., 109, pp. 257-263
[15]Kogut L, and Etsion I, "A finite element based elastic-plastic model for the contact of rough surfaces," STLE Tribol Trans 2003,46, 383-390.
[16]Jackson,R.L., and Green, I., "A Statistical Model of Elasto-plastic Asperity Contact between Rough Surfaces," Tribology International, 39,906-914.
[17]Greenwood, J.A. and Tripp, J.H., 1970, "The Contact of Two Nominally Flat Rough Surfaces," Proc. Instn. Mech. Engrs., Vol.185, pp.625-633.